Available online at www.sciencedirect.com
SCIENCE DIRECT®
Journal of Solid State Chemistry 177 (2004) 1302–1311
JOURNAL OF SOLID STATE CHEMISTRY
http://elsevier.com/locate/jssc

Rare earth phosphate powders $RePO_4 \cdot nH_2O$ (Re = La, Ce or Y)—Part I. Synthesis and characterization

S. Lucas,[a] E. Champion,[a,*] D. Bregiroux,[a,b] D. Bernache-Assollant,[a] and F. Audubert[b]

[a] *Science des Procédés Céramiques et de Traitements de Surface, Université de Limoges, UMR CNRS 6638, 123, Avenue Albert Thomas, 87060 Limoges Cedex, France*

[b] *CEA Cadarache, DEN/DED/SEP/LCC, 13108 Saint Paul lez Durance, France*

Received 22 July 2003; received in revised form 30 October 2003; accepted 6 November 2003

Abstract

Rare earth phosphate powders (Re = La, Ce or Y) were synthesized from an aqueous precipitation method. The effect of temperature, pH, ripening time and Re/P mole ratio of the initial reagents was investigated. Elementary analysis, surface area and bulk density measurements, FT-infrared spectroscopy, X-ray diffraction and SEM observations were performed to characterize the precipitates. All the powders of hydrated form (La, Ce or Y)$PO_4 \cdot nH_2O$ were single phase. They exhibited a Re/P mole ratio smaller than 1 due to residual H_3PO_4 adsorbed at their surface. A unit formula could be written as $RePO_4 \cdot nH_2O \cdot (H_3PO_4)_x$ with $n \approx 0.5$ (for Re = La or Ce) or $n = 2$ (for Re = Y) and $x < 0.1$. High-temperature thermogravimetry was necessary to detect these residuals and insure the purity of the powders. The precipitation of lanthanum or cerium phosphates was slow, resulting in powders with a high specific surface. The precipitation of yttrium phosphate was faster and significant crystal growth occurred during the ripening, which resulted in a whisker-like morphology and a very low specific surface.

Keywords: Rare earth phosphate; Powder synthesis; Rhabdophane; Churchite; Precipitation; Polytrioxophosphate

1. Introduction

Rare earth phosphates ($RePO_4$) have a wide range of potential applications either in the form of powders, coatings or dense sintered parts. They have become of growing interest during the past few years and numerous researches have been devoted to these compounds in the field of ceramic materials for the development of either laminate composites, fiber–matrix interfaces in ceramic matrix composites or thermal protection coatings [1–7]. They were also investigated as potential matrices for the specific conditioning of separated long-lived radionuclides such as trivalent actinides [8,9] or as solid-state protonic conductors [10].

Several authors reported the synthesis of rare earth phosphate compounds via different methods such as wet chemical precipitation, sol–gel, hydrothermal or high-temperature solid-state reactions [11–26]. The physico-chemical properties of the powders, which depend on the synthesis route, i.e., the chemical composition, the crystalline structure, the grain size and the morphology, influence the thermal behavior and the sintering of ceramic materials and therefore their final physico-chemical properties. So, they are of prime importance in the manufacturing processes. But, no study concerned rare earth phosphates through the influence of the synthesis parameters on both the characteristics of the resulting powders and further ceramic processing.

This paper is the first part of a study devoted to the synthesis, characterization and thermal behavior of three rare earth phosphate powders (Re = La, Ce or Y). It is the component of a systematic approach dedicated to the elaboration of $RePO_4$ ceramics that will also concern the sintering behavior and the properties of phosphate-based materials. The present work deals with the synthesis of powders using a wet chemical method and with their characterization. The influence of the synthesis parameters, i.e., the temperature, pH, concentration of the initial reagents and ripening time, on the precipitate characteristics is reported.

*Corresponding author. Fax: +33-555457586.
E-mail address: champion@unilim.fr (E. Champion).

0022-4596/$ - see front matter © 2003 Elsevier Inc. All rights reserved.
doi:10.1016/j.jssc.2003.11.003

2. Materials and methods

2.1. Powder synthesis

The powders were prepared by an aqueous precipitation method from the addition of a rare earth chloride solution ($LaCl_3 \cdot 7H_2O$; $CeCl_3 \cdot 7H_2O$, $YCl_3 \cdot 6H_2O$—Analytical grade, Aldrich, France) into a reactor containing a phosphate solution. Depending on the pH of the synthesis, the phosphating reagent was either phosphoric acid (H_3PO_4, Analytical grade, Aldrich) or diammonium hydrogenphosphate ($(NH_4)_2HPO_4$, Analytical grade, Aldrich). The concentration of the solutions was $0.4\,mol\,L^{-1}$ for a *Re*/P mole ratio of the initial reagents equal to 1. They were fixed at 0.4 and $0.2\,mol\,L^{-1}$ for a *Re*/P ratio of 2:1 and at 0.2 and $0.6\,mol\,L^{-1}$ for a *Re*/P of 1:3. The synthesis device was a fully automated apparatus. The rare earth-containing solution was added, at a rate of $30\,mL\,min^{-1}$, using a peristaltic pump. The pH was maintained at a constant value by the addition of an ammonium hydroxide solution (NH_4OH, analytical grade, Aldrich) using a pH stat (Hanna Instruments, USA). The temperature was controlled and regulated (IKA Labortechnik, Germany). The suspension was continuously stirred and refluxed. After the complete addition of the rare earth solution, the suspension was ripened for various times, then centrifugated. The resulting precipitate was washed with distilled water, centrifugated three times, and finally dried at 80°C. The conditions of synthesis used and the associated precipitate references are summarized in Table 1.

Table 1
Synthesis parameters for various conditions

Reference	pH	Phosphate reagent	Initial *Re*/P (mole ratio)	Temperature (°C)	Ripening time (h)
LaP Tamb	<1	H_3PO_4	1	Ambient	0
LaP T30h00	<1	H_3PO_4	1	30	0
LaP T30h20	<1	H_3PO_4	1	30	20
LaP T50h00	<1	H_3PO_4	1	50	0
LaP T50h20	<1	H_3PO_4	1	50	20
LaP T70h20	<1	H_3PO_4	1	70	20
LaP T80h00	<1	H_3PO_4	1	80	0
LaP T90hxx	<1	H_3PO_4	1	90	0–336
LaP 2:1	<1	H_3PO_4	2/1	Ambient	0
LaP 1:3	<1	H_3PO_4	1/3	Ambient	0
LaP pH3	3	$(NH_4)_2HPO_4$	1	30	0
LaP pH9	9	$(NH_4)_2HPO_4$	1	30	0
CeP T50h20	<1	H_3PO_4	1	50	20
PY T30h00	<1	H_3PO_4	1	30	0
YP T30h01	<1	H_3PO_4	1	30	1
YP T50h00	<1	H_3PO_4	1	50	0
YP T50h01	<1	H_3PO_4	1	50	1
YP T50h02	<1	H_3PO_4	1	50	2
YP T50h05	<1	H_3PO_4	1	50	5
YP T70h00	<1	H_3PO_4	1	70	0
YP T70h01	<1	H_3PO_4	1	70	1

2.2. Powder characterization

X-ray powder diffraction (XRD) patterns were recorded from 10° to 60° with a $\theta/2\theta$ diffractometer (Cu$K\alpha$ radiation, Siemens, Model D5000, Germany). The crystalline phases were determined from the comparison of registered patterns with the International Center for Diffraction Data (ICDD)—Powder Diffraction Files (PDF). Elementary analyses were realized by an inductively coupled plasma method (ICP-MS) in order to determine the *Re*/P mole ratio of the precipitates with a deviation of ± 0.04. Infrared spectra of powders (FTIR) were recorded in the range 400–$4000\,cm^{-1}$ on a Fourier-transform spectrometer (Perkin Elmer, Spectrum 1, USA) with a resolution of $4\,cm^{-1}$. The powder samples were mixed with KBr, then pressed in a 13 mm cylindrical die. Thermogravimetric analyses (TGA), which will be discussed in detail in Part II, were performed up to 1500°C under nitrogen gas flow (TA instruments, model SDT 2960, USA) in order to precise some of the powder properties.

The specific surface area of powders (S_A) was measured by the BET method (analyzer Micromeritics ASAP 2010, USA) after degassing the solid under vacuum at 100°C for 24 h. The bulk density of the powders was measured using helium pycnometry (Micromeritics Accupyc 1330 V2.01, USA). The values, given with a deviation of ± 0.02, were an average of 10 measurements. Scanning electron microscopy (SEM) was used for morphological observations (Philips XL 30, The Netherlands).

3. Results and discussion

3.1. Lanthanum and cerium phosphates

3.1.1. General characteristics of the precipitates

The synthesis of lanthanum and cerium phosphates led to powdered samples with similar physico-chemical properties. Typical XRD patterns of the precipitates are given in Fig. 1. Whatever the synthesis parameters considered, only one crystalline phase was detected. Both La and Ce phosphate powders exhibited a hexagonal structure of the rhabdopphane-type compounds $LaPO_4 \cdot 0.5H_2O$ (ICDD-PDF 46-1439) or $CePO_4 \cdot H_2O$ (PDF 35-0614). The width of the diffraction lines indicated a low crystallinity of this phase. The water content of these hydrated compounds was determined from thermogravimetric analyses. The n values are summarized in Table 2. The hydration was almost constant with $n \approx 0.6$ mol. The elementary analyses led to a *Re*/P mole ratio between 0.90 and 0.96, i.e., lower than the stoichiometric value of 1, which means that the precipitates always contained an excess of phosphorus (or were *Re*-deficient). All the

precipitates exhibited a high specific surface area and the grains were agglomerated needle-like nanosized crystals as shown in the example in Fig. 2 (LaP Tamb). The bulk density of the powders was always lower than the calculated value, i.e., 4.268 (Table 2). Several phenomena are responsible for this result: the presence of synthesis residuals, the relatively low crystallinity of the precipitates and/or the possible presence of closed porosity inside the agglomerates which cannot be excluded too.

FTIR spectra of the precipitates are given in Fig. 3. Most of the bands were characteristic of the vibrations of phosphate groups [27,28]: at about 542, 570 and 615 cm^{-1} for v_4, shoulder at 960 cm^{-1} for v_1, at 1015 and 1050 cm^{-1} for v_3. v_2 is not observed in the investigated range of wavenumbers. The wide bands between 3460 and 3550 cm^{-1} and the band at 1630 cm^{-1} were assigned to H_2O vibrations. The absence of bands of water vibration in the 700–900 cm^{-1} domain indicated a zeolitic nature of the water contained in these compounds [12]. Two additional bands at about 690 and 890 cm^{-1} were not assigned. Such bands could be observed on IR spectra of lanthanum phosphate powders synthesized using a similar wet precipitation method [29]. In early investigations, we hypothesized the presence of HPO_4^{-2} ions, either substituted for PO_4^{3-} in the lanthanide phosphate lattice [30] or adsorbed at the surface of the sample [31]. In this last case, the species must be adsorbed under the neutral form H_3PO_4, as will be explained in the following subsections.

The first assumption was made on the basis of the well-known behavior of calcium phosphate hydroxyapatite ($Ca_{10}(PO_4)_6(OH)_2$), in which hydrogenphosphate ions may substitute phosphate groups during the synthesis by wet route, depending on the pH value [32]. In the presence of HPO_4^{2-}, a band at about 875 cm^{-1} assigned to hydrogenphosphate P–O–H

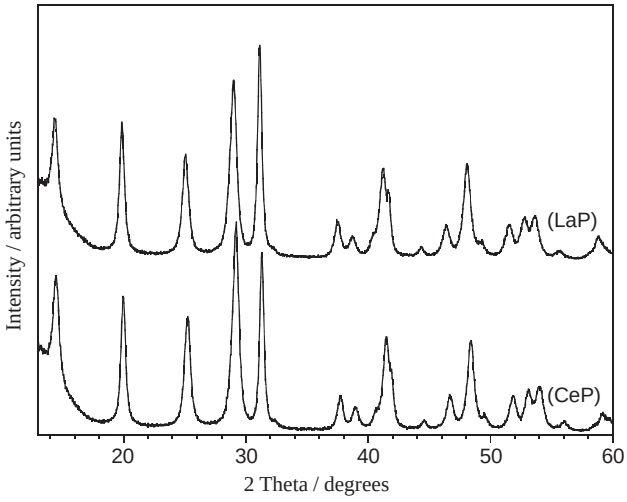

Fig. 1. XRD diagrams of lanthanum and cerium phosphate precipitates LaP T50h20 (PDF 46-1439) and CeP T50h20 (PDF 35-0614).

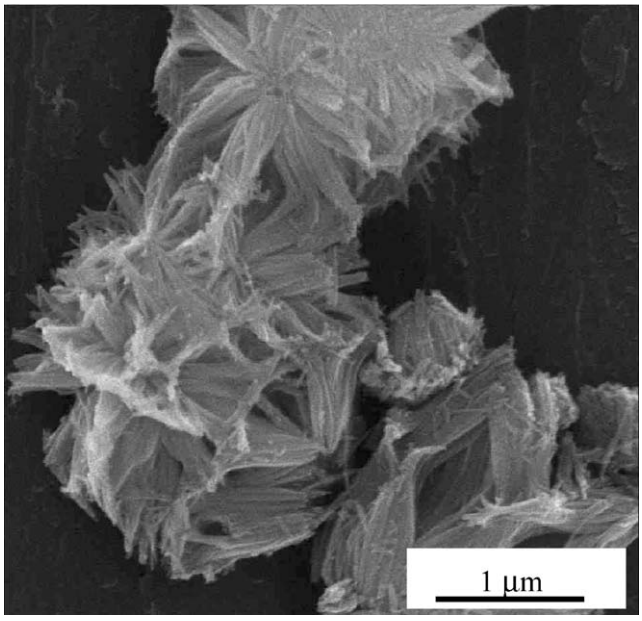

Fig. 2. SEM micrograph of lanthanum phosphate precipitate (LaP Tamb).

Table 2
Main characteristics of lanthanum and cerium phosphate precipitates

Reference	Reaction yield (%)	S_A ($m^2 g^{-1}$)	Bulk density	*Re*/P (mole ratio)	H_2O (mol)	$Re(PO_3)_3$ (wt%)
LaP Tamb	59	78.4±0.4	3.90	0.90	0.61	2.18
LaP T30h00	66	76.7±0.5	3.85			
LaP T30h20	91	74.6±0.2	4.04			
LaP T50h00	80	55.1±0.2	3.98			
LaP T50h20	≈100	68.8±0.3	3.98	0.94	0.57	1.62
LaP T70h20	≈100	63.6±0.4	3.97			
LaP T80h00	≈100	64.5±0.6	3.91		0.61	1.24
LaP 2:1		80.6±0.6	3.77	0.93	0.63	1.15
LaP 1:3		67.5±0.4	4.08		0.57	2.40
LaP pH3		97.6±0.5	3.59			2.44
LaP pH9		80.2±0.7	3.28			3.10
CeP T50h20		69.0±1.0	4.16	0.96	0.6	1.11

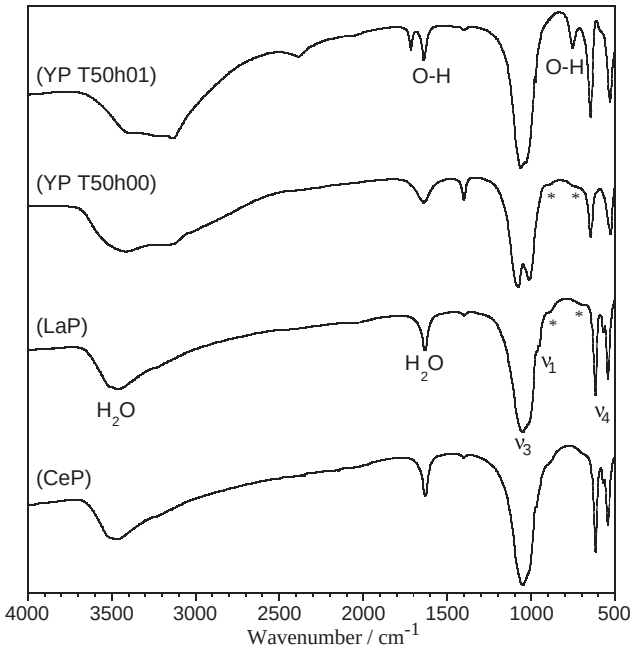

Fig. 3. FTIR spectra of lanthanum (LaP T30h00), cerium (CeP T50h20) and yttrium (YP T50h00 and YP T50h01) phosphate precipitates.

stretching mode appears on the IR spectrum of the substituted hydroxyapatite [33]. As for hydroxyapatite, a hydrogenphosphate substitution in the rare earth phosphate lattice should lead to non-stoichiometric *Re*-deficient compounds in order to preserve the electroneutrality. A chemical composition could be written as follows:

$$Re_{1-0.33y}(PO_4)_{1-y}(HPO_4)_y \cdot xH_2O$$

Recently, Kijkowska [34] stated the same hypothesis and argued that, as it is the case of hydroxyapatite, hydrogenphosphate would condensate into diphosphate $P_2O_7^{4-}$ above 500°C. Nevertheless, at the sight of the thermal behavior of the powders (detailed in Part II of this study), diphosphates were never detected in the powder whatever the temperature considered. Finally, it appeared that the most convincing hypothesis was the adsorption of hydrogenphosphate species at the surface of the rare earth phosphate powders inducing an excess of phosphorus and a *Re*/P mole ratio smaller than 1 as determined from elementary analyses. Several attempts to remove these residuals by successive water washing steps were unsuccessful.

The presence of such absorbed residuals was also confirmed and quantified using high-temperature thermogravimetric analysis. The phenomena exposed hereafter summarize the necessary results for a good understanding; much more details can be found in Part II of this study devoted to the thermal behavior. The method used for the quantification is based on the thermal formation of a lanthanum polytrioxophosphate $Re(PO_3)_3$ at about 950°C as secondary phase resulting from the adsorbed H_3PO_4 followed by its decomposition between 1050°C and 1350°C with P_4O_{10} gas release according to the following reaction:

$$2Re(PO_3)_{3(solid)} \rightarrow 2RePO_{4(solid)} + P_4O_{10(gas)}\uparrow \quad (1)$$

The amount of $Re(PO_3)_3$ was determined from the weight loss recorded between 1050°C and 1350°C that accompanied its decomposition, as shown in Fig. 4. This amount was determined versus the specific surface area of lanthanum phosphate powders synthesized at 90°C during various ripening times (Fig. 5). Indeed, it was directly proportional to the specific surface area of the powder. This confirms that the hydrogenphosphate species are located at the surface of the precipitates. In order to precise their chemical nature, a pH titration using NaOH solution was performed on a solution containing 2 g of a washed precipitate (LaP T30h00) stirred in 40 mL of deionized water. The titration plot was typically that of a phosphoric acid dilute solution with an initial pH of 2.55 ± 0.05 (Fig. 6) and it can be concluded that H_3PO_4 is the adsorbed species. The pH of the first neutralization point, which corresponds to the first maximum of the derivative plot, was 4.5 (against 4.65 considering $pKa_1 = 2.1$ and $pKa_2 = 7.2$ for the phosphoric acid) and the pH of the second one was 8.9 (theoretically 9.75 using $pKa_3 = 12.3$). The apparent discrepancy between the experimental data and calculated values comes from two different phenomena. First, the NaOH solution was not degassed and the titration was performed under air. The presence of residual hydrogencarbonate ($pKa_1 = 6.3$) naturally dissolved in water modifies the titration curve lightly. A second and more convenient explanation comes from the fact that this experiment is not a classical titration of acidic species in solution. Indeed, the adsorbed species must be

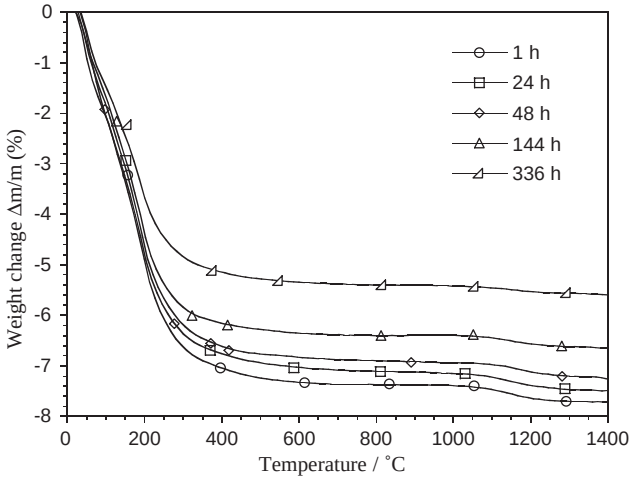

Fig. 4. TGA of lanthanum phosphate precipitates synthesized at 90°C for various ripening times.

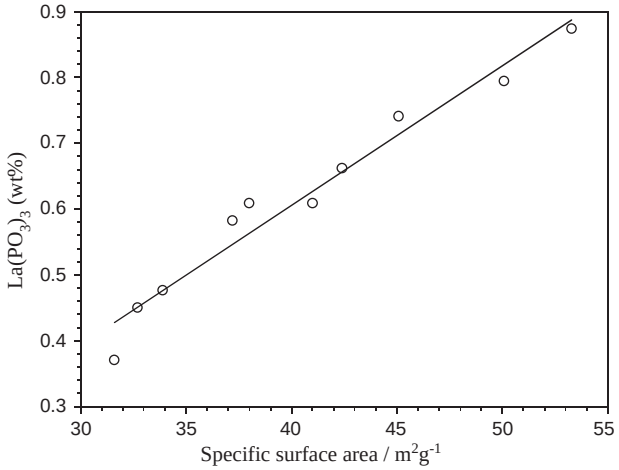

Fig. 5. Amount of lanthanum polytrioxophosphate high-temperature secondary phase $La(PO_3)_3$ versus the specific surface area of lanthanum phosphate precipitates (synthesized at 90°C and pH < 1).

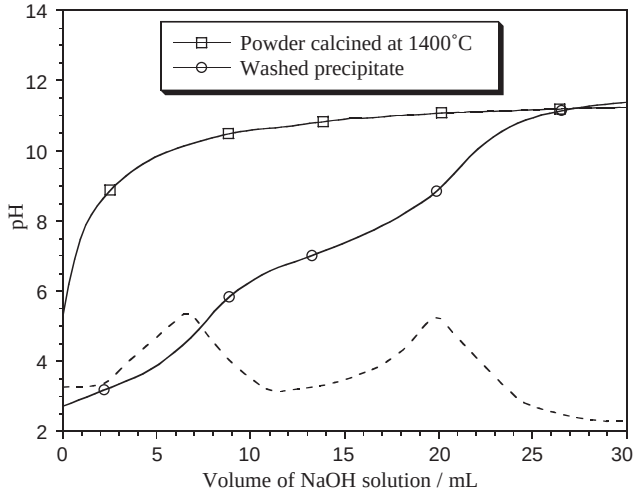

Fig. 6. NaOH titration plots of LaP T30h00 washed precipitate (NaOH = 0.05 M), and its derivative curve (dashed line), and of La T30h00 powder calcinated at 1400°C for 1 h (NaOH = 0.01 M).

released from the surface of the solid. Considering that the powder (LaP T30h00) contains 0.1 mol of adsorbed H_3PO_4 (which corresponds to $Re/P = 0.91$), 2 g of this powder contains about 8×10^{-4} mol of H_3PO_4. Consequently, on the hypothesis of a total release the 40 mL of solution used in the experiment should have a H_3PO_4 concentration of $0.02\,mol\,L^{-1}$. The values calculated from the titration data give a H_3PO_4 concentration of $4 \times 10^{-3}\,mol\,L^{-1}$ for the initial pH (2.55), $8 \times 10^{-3}\,mol\,L^{-1}$ at the first endpoint (with $V_{NaOH} = 6.5\,mL$) and $1.7 \times 10^{-2}\,mol\,L^{-1}$ at the second endpoint (with $V'_{NaOH} = 20-6.5\,mL$). These results would indicate a progressive release of adsorbed H_3PO_4 with the addition of hydroxide ions in the solution containing the powder. Finally, it could be assessed that desorption in solution should be associated to an equilibrium, which is displaced during the titration.

After the calcination of the powder at 1400°C for 1 h that allowed the removal of the adsorbed H_3PO_4, the titration plot did not exhibit any acidic species in the solution. The lightly acidic initial pH of 5.3 is mainly due to the presence of the residual hydrogencarbonate. Thus, it can be hypothesized that the adsorbed species were either in the form of residual H_3PO_4 or $NH_4H_2PO_4$ in the dried precipitates, depending on the synthesis conditions, i.e., on the nature of the initial phosphate-containing reagent (Table 1). During heating, they would lead to the formation of $Re(PO_3)_3$ according to the following reactions:

$$2H_3PO_{4(adsorbed)} + RePO_{4(solid)} \rightarrow Re(PO_3)_{3(solid)} + 3H_2O_{(gas)}\uparrow \quad (2)$$

$$2NH_4H_2PO_{4(ad)} + RePO_{4(solid)} \rightarrow Re(PO_3)_{3(s)} + 3H_2O_{(gas)}\uparrow + 2NH_{3(gas)}\uparrow \quad (3)$$

The detection threshold of polytrioxophosphate secondary phase was investigated through different methods. The results obtained from FTIR spectroscopy and Raman spectroscopy were similar with a detection threshold of the hydrogenphosphate vibrations corresponding to about 1 wt% of the associated $Re(PO_3)_3$ phase (see also comment of Fig. 3 in Section 3.2). For XRD, the detection threshold was about 2 wt% using a good resolution pattern. This result is illustrated in the diagrams in Fig. 7 where the main diffraction peak at $2\theta \approx 24.1°$ of the secondary phase $La(PO_3)_3$ present in a lanthanum phosphate powder heat treated at 1000°C was rarely detected when the amount was below this limit of 2 wt%. Finally, neither IR nor Raman spectroscopy nor XRD is able to insure the purity of a rare earth phosphate powder. High-temperature thermogravimetry was thus required since it allows the detection of very small weight changes (with usual precision of 0.1 wt%). This is all the more important in the field of ceramic materials processing since secondary phases may have major consequences either on the elaboration or on the properties of the final material. For example, it can act as a sintering aid, and enhance or prevent grain growth. In this field, the role of rare earth polytrioxophosphates as a minor secondary phase will be discussed in a forthcoming paper.

3.1.2. *Influence of synthesis parameters*

The influence of the synthesis parameters was investigated on the lanthanum phosphate precipitates. The main results are summarized in Table 2. The yield of the precipitation reaction was determined versus the temperature and ripening time without any pH regulation of the solution. The precipitation reaction was

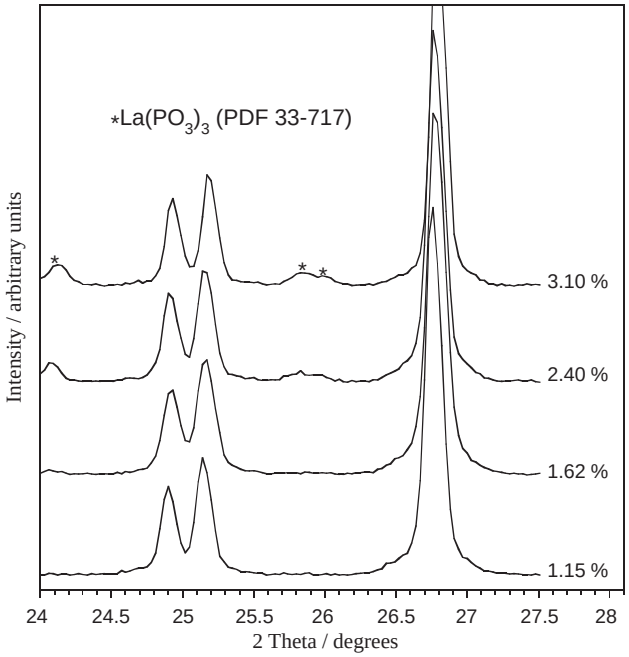

Fig. 7. XRD diagrams (step size: 0.03°, counting time: 30 s) of lanthanum phosphate powders calcinated at 1000°C for 2 h and containing various amounts of residual lanthanum polytrioxophosphate (determined from TGA).

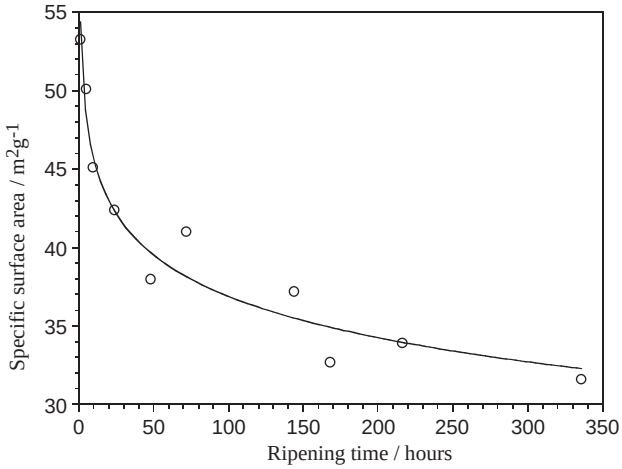

Fig. 8. Specific surface area of lanthanum phosphates precipitated at 90°C and pH < 1 versus the ripening time.

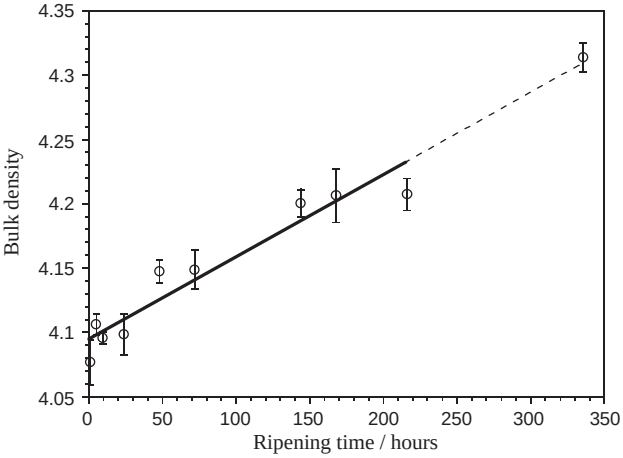

Fig. 9. Bulk density of $LaPO_4 \cdot nH_2O$ precipitated at 90°C and pH < 1 versus the ripening time.

thermally activated and it was complete after 20 h ripening at 50°C. A decrease of the ripening time required temperatures of at least 80°C to obtain quantitative the precipitation. For syntheses at pH < 1, the specific surface area of the powders decreased slightly with the temperature. But, in any case it remained high (with values higher than $60\,m^2\,g^{-1}$). The effect of the ripening on the reduction of the specific surface area became significant only at high temperatures and for a very long time (as shown in Fig. 8 for syntheses performed at 90°C). Nevertheless, the surface remained high. The values were above $30\,m^2\,g^{-1}$, even after 2 weeks (336 h) of ripening at 90°C. The bulk density, although remaining always below the calculated value of 4.268 for the rhabdophane-type hexagonal structure, increased slowly with the ripening time to reach values close to 4.20 from about 150 h at 90°C (Fig. 9). The value of 4.31 ± 0.02, i.e., superior to the theoretical value of 4.268, determined for the precipitate ripened for 336 h can be explained by the presence of monoclinic anhydrous monazite-type $LaPO_4$ (PDF 32-0943) in this precipitate, as detected on its XRD pattern (Fig. 10), whose calculated bulk density is 5.067. These data were not included in the linear regression (Fig. 9). The formation of anhydrous monazite in long-duration syntheses was already reported by Hikichi [14]. The presence of monazite or rhabdophane was also reported by Terra et al. [26]. During the ripening, a variation of the hydration ratio of the hydrated rhabdophane-type phosphate was also registered on the TGA curves (Fig. 4). Fig. 11 shows that it decreased slightly from about $n = 0.65$ without ripening down to $n = 0.5$ mol after a 336 h ripening. This last value corresponded to the theoretical one given for the La-rhabdophane structure ($n = 0.5$). Nevertheless, it must be noted that for this very long ripening time the presence of anhydrous $LaPO_4$ as a second phase also contributes to the decrease of the hydration ratio. These data were not included in the linear regression. Finally, the crystallinity of the hydrated precipitates appeared to increase slowly with ripening at high temperatures.

A change of the reagents stoichiometry from La/P = 1/3 up to 2 did not affect its nature, $LaPO_4 \cdot nH_2O$ is always the less soluble compound that precipitates. One of the main effects of the synthesis parameters on the properties of the precipitate is due to the pH of the synthesis. Increasing pH value induced a drastic

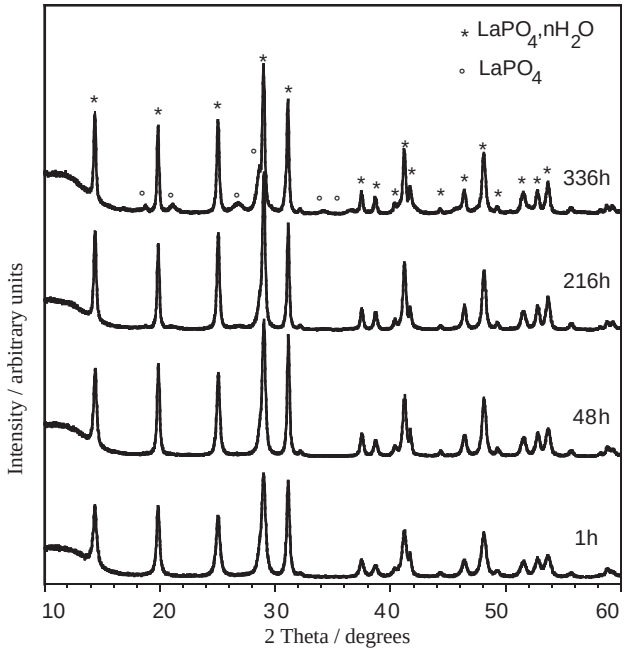

Fig. 10. XRD diagrams of lanthanum phosphate precipitates synthesized at 90°C, pH < 1 for various ripening times.

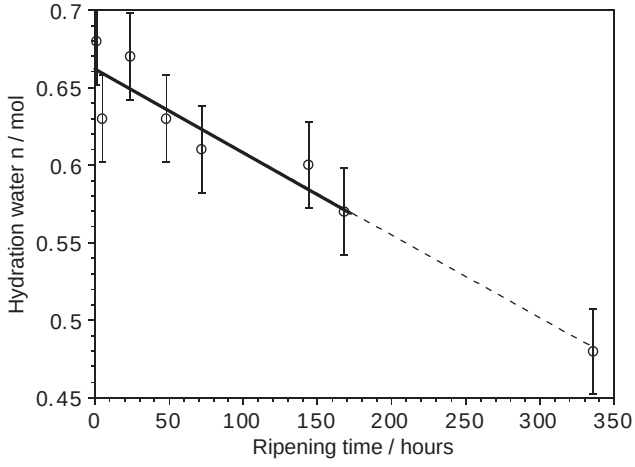

Fig. 11. Hydration water in the $LaPO_4 \cdot nH_2O$ precipitates synthesized at 90°C and pH < 1 versus the ripening time.

decrease of the precipitate crystallinity as illustrated by the broadening of the diffraction peaks observed at pH = 9 (Fig. 12). It must be noted that this phenomenon should not result from a decrease of the particle size, which is also known to lead to a broadening of the diffraction lines, since the specific surface area and the powder morphology remained similar in comparison with the powders synthesized in an acidic medium. This decrease of the crystallinity is logically accompanied by lower bulk densities of the powders (Table 2). To a less extent, a small sharpening of the diffraction peaks appeared at low synthesis temperatures, also indicating

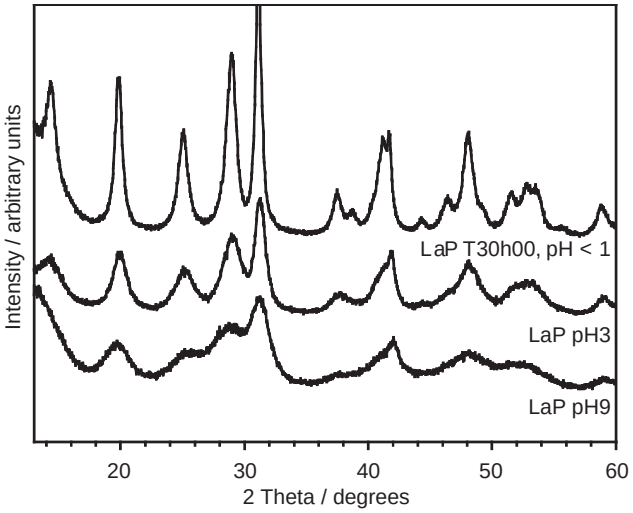

Fig. 12. XRD diagrams of lanthanum phosphate precipitates synthesized at 30°C and different pH values, without ripening.

a lower crystallinity of the powders. This was more particularly visible with the three peaks in the 2θ range 50–55°. Another phenomenon was associated to the peak located at $2\theta = 41.8°$ (003). At low temperatures and without ripening, the relative intensity of this peak was greater than that expected. For a comparison, the relative intensities should be 39% and 26% for the peak (211) at $2\theta = 41.3°$ and for the peak (003) at $2\theta = 41.8°$, respectively. This may indicate an anisotropic behavior of the crystal formation during the first stages of the precipitation process. This may be linked to the needle-like morphology of crystals precipitated at low temperatures without ripening (Fig. 2). Then, at high temperatures or after 20 h ripening, the grain would have grown more isotropically on account of the evolution of the relative intensities of these diffraction peaks, which again become normal. This may be confirmed by the morphology of the powders synthesized at high temperatures without ripening (Fig. 13a) or after 20 h ripening (Fig. 13b). The needle-like morphology of the crystals was less observable than for syntheses at low temperatures and agglomerates appeared coarser and denser compared to the morphology of the low-temperature precipitates.

FTIR spectra of the powders precipitated in the different synthesis conditions and the characteristics of hydrated lanthanum phosphate compounds were similar (Fig. 14). There were only some additional bands registered in the range 1400–1460 cm^{-1} and at 3120 cm^{-1} on the spectrum of the powder synthesized at pH = 9 that were assigned to N–H vibrations resulting from the presence of ammonium synthesis residues in the precipitates.

The modification of the synthesis parameters also influenced the amount of H_3PO_4 (or $NH_4H_2PO_4$) adsorbed at the particles surface. This amount, reported

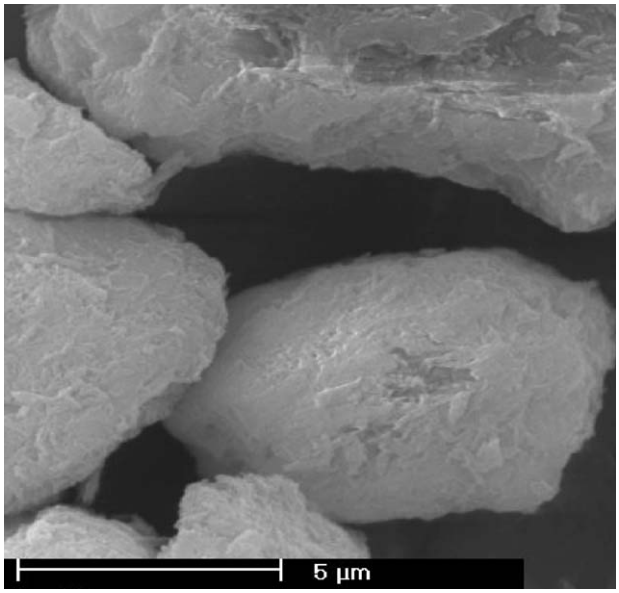

(a) 80°C, without ripening (LaP T80h00).

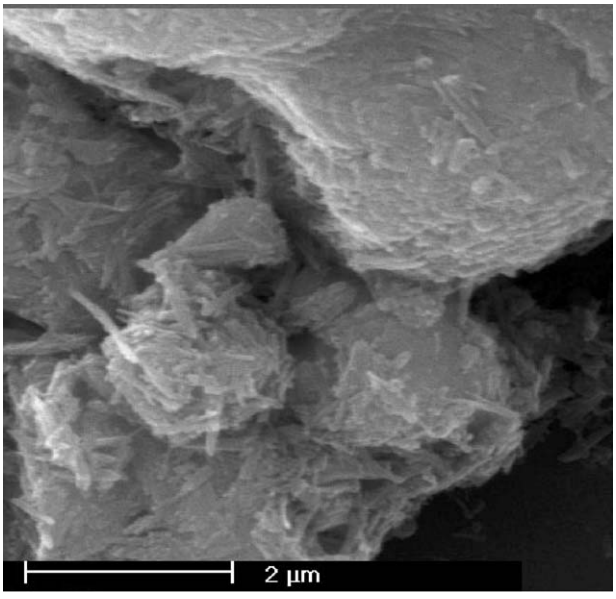

(b) 50°C, 20 h ripening (LaP T50h20).

Fig. 13. SEM micrographs of lanthanum phosphate precipitates synthesized at pH < 1: (a) 80°C, without ripening (LaP T80h00), and (b) 50°C, 20 h ripening (LaP T50h20).

in Table 2 as its associated $Re(PO_3)_3$ high-temperature secondary phase, indicates that increasing the pH of the synthesis or decreasing the La/P ratio of the initial reagents increased the quantity of adsorbed species at the surface of the powder. These changes must be dissociated from the effect of the surface area of the above-mentioned powders because the values varied from 1.15 (LaP 2:1) to 2.4 (LaP 1:3) and 3.10 wt% (LaP pH 9) while the specific surface areas of these powders were 80.6 ± 0.6, 67.5 ± 0.4 and $80.2 \pm 0.7\ m^2\ g^{-1}$, respectively.

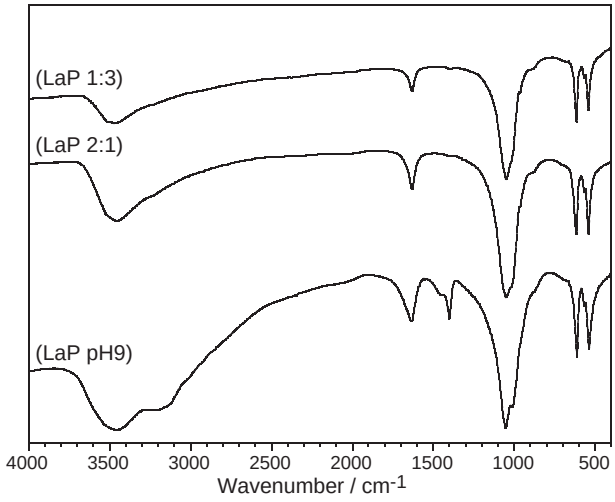

Fig. 14. FTIR spectra of lanthanum phosphates precipitated from different synthesis conditions without ripening.

3.2. Yttrium phosphates

The precipitation of yttrium phosphates was different from that of lanthanum or cerium phosphate. XRD diagrams of the precipitates synthesized at 50°C for various ripening times are given in Fig. 15. After 1 h ripening, the precipitates were well crystallized. The crystalline phase was hydrated yttrium phosphate of monoclinic structure ($YPO_4 \cdot 2H_2O$, churchite-like compound). Without any ripening, the powder was mainly amorphous, and only the most intense peaks of the crystalline phase were detected on the XRD diagram. The amorphous phase seemed to be related to the tetragonal structure of the anhydrous YPO_4 phase, whose theoretical pattern is also reported in Fig. 15.

FTIR spectra of the same powders are shown in Fig. 3. As for lanthanum and cerium phosphates, the spectra exhibited all the bands assigned to the vibrations of PO_4 groups. Concerning the water vibrations, in addition to the wide bands in the region 3000–3700 cm^{-1}, the presence of two bands at 1640 and 1713 cm^{-1} and the band at 748 cm^{-1} was characteristic of coordinated water in the precipitates synthesized with ripening [35]. Without ripening only one band was detected at around 1650 cm^{-1} and the band at 750 cm^{-1} did not appear. This indicates that in the amorphous compound, the water was less coordinated. The hydration of the precipitates hypothesized as $YPO_4 \cdot nH_2O$ was $n \approx 1.2$ without ripening and $n = 2$ from 1 h ripening. This last value corresponds to the theoretical formula of the crystallized hydrated yttrium phosphate of monoclinic structure. Therefore, the amorphous compound appears only partially hydrated with a structure close to that of the tetragonal anhydrous phosphate. Without ripening, the two bands at about 690 and 890 cm^{-1} attributed to hydrogenphosphate vibrations in lanthanum and cerium

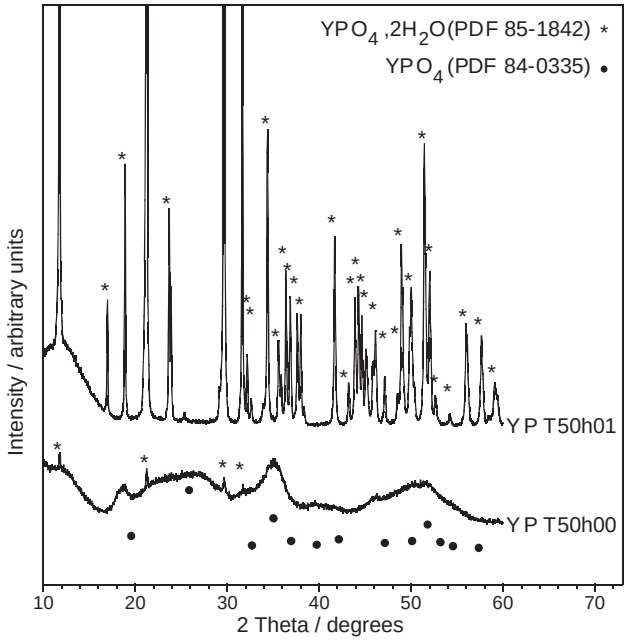

Fig. 15. XRD diagrams of yttrium phosphate precipitates synthesized at 50°C without ripening (YP T50h00) and after 1 h ripening (YP T50h01).

phosphates were also detected in the precipitate whereas they were no longer present after 1 h ripening. For these syntheses at 50°C, the surface area of the powder was $105 \pm 1\,m^2\,g^{-1}$ without ripening and dropped down to $1.95 \pm 0.03\,m^2\,g^{-1}$ after 1 h ripening. On the hypothesis that H_3PO_4 would be adsorbed at the particle surface, the disappearance of vibration bands could be explained by this great change of specific surface area. The decrease of the amount of adsorbed species was confirmed by the increase of the Y/P mole ratio from 0.93 to 0.95 and the decrease of the amount of yttrium polytrioxophosphate secondary phase $Y(PO_3)_3$ associated with them from 1.4 wt% down to 0.80 wt% for these same powders, respectively. The important modifications of the powder characteristics during the ripening were also accompanied by a morphological modification of the precipitated particles. SEM observations of the precipitates (Fig. 16) showed a rapid growth of these particles. They were spherical-like of size inferior to 50 nm at 50°C without ripening (Fig. 16a) and needle-like of more than 5 μm length after only 1 h ripening (Fig. 16b). The bulk density of the amorphous precipitates was about 2.95. It increased up to 3.18 ± 0.02 for the ripened and crystallized precipitates, a value that corresponds to the calculated one for hydrated yttrium phosphate of monoclinic structure (3.185).

From these results it can be stated that the synthesis of well-crystallized yttrium phosphate precipitates of monoclinic structure is kinetically rapid. This was not the case for lanthanum or cerium phosphates.

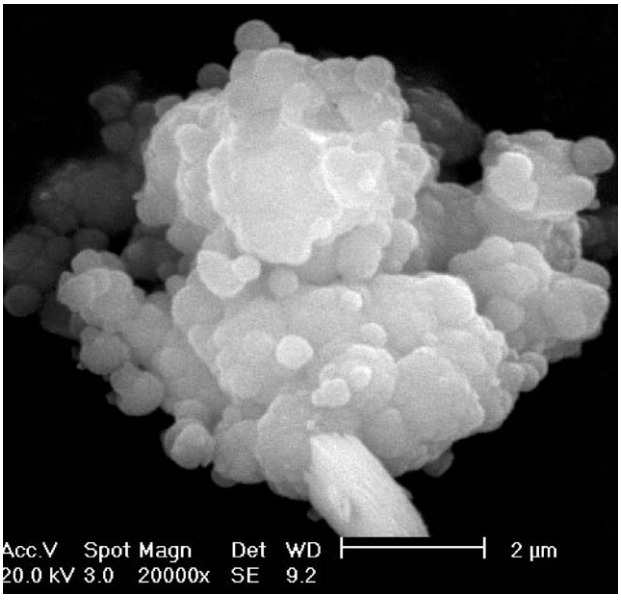

(a) Without ripening (YP T50h00)

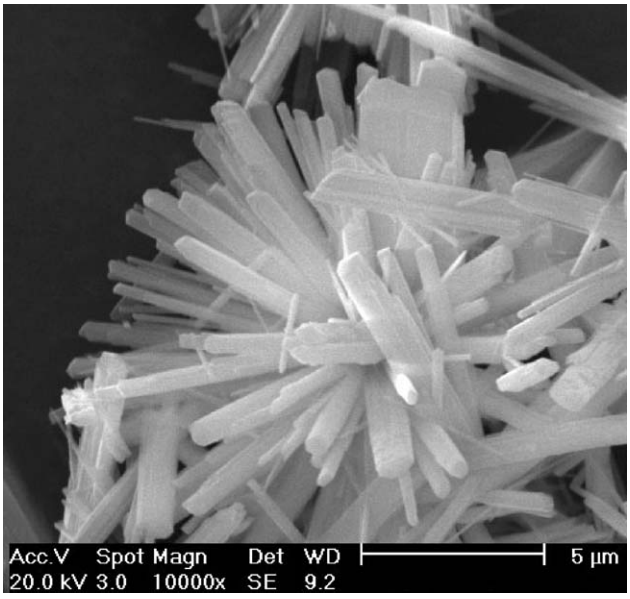

(b) After 1 h ripening (YP T50h01)

Fig. 16. SEM micrographs of yttrium phosphate precipitates synthesized at 50°C and pH < 1: (a) without ripening (YP T50h00), and (b) after 1 h ripening (YP T50h01).

4. Conclusion

The wet synthesis of rare earth phosphates by the precipitation method always leads to the formation of $RePO_4 \cdot nH_2O$ compounds (Re = La, Ce or Y). The stoichiometry of the initial reagents does not influence the chemical composition of the precipitate.

For Re = La or Ce, the precipitation reaction exhibits low kinetic and requires a high temperature of 80°C or ripening during at least 20 h to reach a quantitative yield

of precipitation. About 1 week ripening at 90°C was required to prepare well-crystallized compounds (i.e., with values of the bulk density and a hydration ratio close to the calculated values). The pH of the synthesis influences mainly the crystallinity of the precipitate and the amount of synthesis residuals. The precipitates crystallized in the hexagonal structure of rhabdophane $Re PO_4 \cdot 0.5H_2O$. The ratio of hydration water can vary slightly and this water is of zeolitic nature. The particles are always nanometric with a high specific surface area.

For $Re = Y$, the precipitate is $YPO_4 \cdot 2H_2O$ with a monoclinic structure (churchite-type). The hydration water is coordinated and the behavior during the synthesis differs slightly from that of lanthanum or cerium phosphate. The kinetic of precipitation is accompanied by a rapid crystal growth resulting in the preparation of needle-like crystals of low specific surface area from 1 h ripening even at a low temperature (30°C).

Whatever the conditions of synthesis, H_3PO_4 adsorbed at the surface of the particles is always present in the precipitates. The amount of this residual, although remaining low, is proportional to the specific surface area of the precipitate and is increased by an increase of the synthesis pH or a decrease of the Re/P mole ratio of the initial reagents.

Finally, from these results a unit chemical formula can be proposed as follows:

$$Re PO_4 \cdot nH_2O \cdot (H_3PO_4)_x$$

with $n \approx 0.5$ (Re = La or Ce), $n = 2$ (Re = Y) and $0 < x < 0.1$ ($Re/P > 0.9$).

Further elaboration of ceramic materials from such powders could be greatly influenced by the residual species, although their detection can be very difficult when present in a very low amount. To this end, the use of high-temperature thermogravimetry is required and their removal is only possible using a high-temperature calcination treatment at 1400°C in order to get their decomposition.

References

[1] J.B. Davis, D.B. Marshall, P.E.D. Morgan, J. Eur. Ceram. Soc. 20 (2000) 583–587.
[2] P.E.D. Morgan, D.B. Marshall, Mater. Sci. Eng. A 162 (1993) 15–25.
[3] D.H. Kuo, W.H. Kriven, J. Am. Ceram. Soc. 78 (1995) 3121–3124.
[4] E. Boakye, M.D. Petry, R.S. Hay, Ceram. Eng. Sci. Proc. 17 (1996) 53–60.
[5] D.H. Kuo, W.H. Kriven, J. Am. Ceram. Soc. 80 (1997) 2987–2996.
[6] J.B. Davis, D.B. Marshall, K.S. Oka, R.M. Housley, P.E.D. Morgan, Composites: Part a 30 (1999) 483–488.
[7] M.H. Lewis, A. Tye, E.G. Butler, P.A. Doleman, J. Eur. Ceram. Soc. 20 (2000) 639–644.
[8] G.J. McCarthy, W.B. White, D.E. Pfoertsch, Mater. Res. Bull. 13 (1978) 1239–1245.
[9] C. Guy, F. Audubert, J.E. Lartigue, C. Latrille, T. Advocat, C. Fillet, C. R. Acad. Sci. Paris Phys. 3 (2002) 827–837.
[10] T. Norby, N. Christiansen, Solid State Ionics 77 (1995) 240–243.
[11] R.S. Feigelson, J. Am. Ceram. Soc. 47 (1964) 257–258.
[12] J.D. Donaldson, A. Hezel, S.D. Ross, J. Inorg. Nucl. Chem. 29 (1967).
[13] N.N. Chudinova, L.P. Shklover, G.M. Balagina, Inorg. Mater. 11 (1975) 590–593.
[14] Y. Hikichi, K. Hukuo, J. Shiokawa, Bull. Chem. Soc. Japan 51 (1978) 3645–3646.
[15] M.M. Abraham, L.A. Boatner, D.K. Thomas, M. Rappaz, Radioactive Waste Management 1 (1980) 181–191.
[16] Y. Hikichi, Mineral. J. 15 (1991) 268–275.
[17] N. Arul-Dhas, K.C. Patil, J. Alloys Compounds 202 (1993) 137–141.
[18] Y. Guo, P. Woznicki, A. Barkatt, E. Saad, I.G. Talmy, J. Mater. Res. 11 (1996) 639–649.
[19] Y. Fujishiro, H. Ito, T. Sato, A. Okuwaki, J. Alloys Compounds 252 (1997) 103–109.
[20] P. Chen, T.I. Mah, J. Mater. Sci. 32 (1997) 3863–3867.
[21] I.W. Lenggoro, B. Xia, H. Mizushima, K. Okuyama, N. Kijima, Mater. Lett. 50 (2001) 92–96.
[22] L. Bo, S. Liya, L. Xiaozhen, Z. Shuihe, Z. Yumei, W. Tianmin, Y. Sasaki, K. Ishii, Y. Kashiwaya, H. Takahashi, T. Shibayama, J. Mater. Sci. Lett. 20 (2001) 1071–1075.
[23] H. Onoda, H. Nariai, H. Maki, I. Motooka, Mater. Chem. Phys. 78 (2002) 400–404.
[24] R. Kijkowska, J. Mater. Sci. 38 (2003) 229–233.
[25] A.S. Celebi, J.W. Kolis, J. Am. Ceram. Soc. 85 (2002) 253–254.
[26] O. Terra, N. Clavier, N. Dacheux, R. Podor, New J. Chem. 27 (2003) 957–967.
[27] H. Assaaoudi, A. Ennaciri, A. Rulmont, M. Harcharras, Phase Transitions 72 (2000) 1–13.
[28] A. Hezel, S.D. Ross, Spectrochim. Acta 22 (1966) 1949–1961.
[29] H. Assaaoudi, A. Ennaciri, A. Rulmont, Vibrational Spectros. 25 (2001) 81–90.
[30] C. Penot, E. Champion, P. Goursat, Phosphorus Res. Bull. 10 (1999) 308–312.
[31] S. Lucas, E. Champion, C. Penot, G. Leroy, D. Bernache-Assollant, Key Eng. Mater. 206–213 (2002) 47–50.
[32] S. Raynaud, E. Champion, D. Bernache-Assolllant, P. Thomas, Biomaterials 23 (2002) 1065–1072.
[33] J.C. Heughebaert, Thesis, Institut National Polytechnique, Toulouse, 1977.
[34] R. Kijkowska, E. Cholewka, B. Duszak, J. Mater. Sci. 38 (2003) 223–228.
[35] J. Fujita, K. Nakamoto, M. Kobayashi, J. Am. Chem. Soc. 78 (1956) 3963–3965.